Bioactive Materials 28 (2023) 12–26

Contents lists available at ScienceDirect

Bioactive Materials

journal homepage: www.keaipublishing.com/en/journals/bioactive-materials

Intrinsically bioactive and biomimetic nanoparticle-derived therapies alleviate asthma by regulating multiple pathological cells

Jiajun Cai [a,1], Hui Tao [b,1], Huan Liu [a,1], Yi Hu [a], Songling Han [c], Wendan Pu [a], Lanlan Li [d], Gang Li [a], Chenwen Li [a], Jianxiang Zhang [a,c,*]

[a] Department of Pharmaceutics, College of Pharmacy, Third Military Medical University (Army Medical University), Chongqing, 400038, PR China
[b] Department of Pharmacology, College of Pharmacy, Third Military Medical University (Army Medical University), Chongqing, 400038, PR China
[c] State Key Laboratory of Trauma, Burns and Combined Injury, Third Military Medical University (Army Medical University), Chongqing, 400038, PR China
[d] Department of Pharmaceutical Analysis, College of Pharmacy, Third Military Medical University (Army Medical University), Chongqing, 400038, PR China

ARTICLE INFO

Keywords:
Neutrophilic asthma
Nanotherapy
Neutrophil extracellular traps
Inflammasome
Precision therapy

ABSTRACT

Asthma is a serious global public health concern. Airway neutrophilic inflammation is closely related to severe asthma, for which effective and safe therapies remain to be developed. Here we report nanotherapies capable of simultaneously regulating multiple target cells relevant to the pathogenesis of neutrophilic asthma. A nanotherapy LaCD NP based on a cyclic oligosaccharide-derived bioactive material was engineered. LaCD NP effectively accumulated in the injured lungs of asthmatic mice and mainly distributed in neutrophils, macrophages, and airway epithelial cells after intravenous or inhalation delivery, thereby ameliorating asthmatic symptoms and attenuating pulmonary neutrophilic inflammation as well as reducing airway hyperresponsiveness, remodeling, and mucus production. Surface engineering via neutrophil cell membrane further enhanced targeting and therapeutic effects of LaCD NP. Mechanistically, LaCD NP can inhibit the recruitment and activation of neutrophils, especially reducing the neutrophil extracellular traps formation and NLRP3 inflammasome activation in neutrophils. Also, LaCD NP can suppress macrophage-mediated pro-inflammatory responses and prevent airway epithelial cell death and smooth muscle cell proliferation, by mitigating neutrophilic inflammation and its direct effects on relevant cells. Importantly, LaCD NP showed good safety performance. Consequently, LaCD-derived multi-bioactive nanotherapies are promising for effective treatment of neutrophilic asthma and other neutrophil-associated diseases.

1. Introduction

Asthma is a serious global public health concern, which occurs in both children and adults, affecting approximately 339 million people worldwide [1]. Asthma, a heterogeneous chronic inflammatory disease in the airways, is featured by infiltration of inflammatory cells, airway hyperresponsiveness (AHR), airway remodeling, and mucus production. In the pathogenesis of asthma, many cells are involved, including eosinophils, neutrophils, macrophages, mast cells, T lymphocytes, airway epithelial cells, and smooth muscle cells (SMCs) [2]. Generally, it has been considered that asthma (in particular, allergic asthma) is mainly associated with eosinophilic inflammation that can be effectively treated with inhaled corticosteroids [2,3]. However, increasing evidence has shown strong associations of airway neutrophilic inflammation with severe asthma that is resistant to corticosteroid therapy [4,5]. More than 50% of asthma is resulting from non-eosinophilic inflammation, in which neutrophilic inflammation is predominant [6,7]. Neutrophilic asthma (NA) is closely related to persistent, severe, and fatal asthma phenotypes [4,8]. Whereas the standard pharmacological treatment with corticosteroids represents the best therapeutic option for most asthmatic patients, NA remains poorly controlled by available therapies [2,4,9].

Compared to patients with mild asthma, more neutrophils were detected in the airways of severe asthmatics [7,8], suggesting that

Peer review under responsibility of KeAi Communications Co., Ltd.
* Corresponding author. Department of Pharmaceutics, College of Pharmacy, Third Military Medical University, 30 Gaotanyan Main Street, Chongqing, 400038, PR China.
E-mail addresses: jxzhang@tmmu.edu.cn, jxzhang1980@gmail.com (J. Zhang).
[1] These authors contributed equally.

https://doi.org/10.1016/j.bioactmat.2023.04.023
Received 29 October 2022; Received in revised form 20 March 2023; Accepted 24 April 2023

neutrophils most likely play an important role in the pathophysiology of NA [4]. Under normal conditions, neutrophils are first recruited to inflammatory sites and defense against pathogens by phagocytosis, degranulation, and releasing neutrophil extracellular traps (NETs) that are complexes of extracellular DNA fibers, histones, and granular proteins [10]. Also, neutrophils have been implicated in the pathogenesis of many acute/chronic inflammatory disorders [11], in which recruitment and subsequent activation of neutrophils are crucial for the development of a diverse array of diseases [10]. Interleukin (IL)-8, a critical chemokine for neutrophils, was found to be notably increased in NA patients, which can be released by epithelial cells and infiltrated neutrophils in the lungs to participate in airway inflammation [12]. Additionally, NETs generated from activated neutrophils can cause airway injury due to direct cytotoxicity to pulmonary epithelial cells, thus promoting severe inflammation in NA [13,14]. Importantly, NETs were found in the airways of a subset of patients with more severe asthma [15]. Reversible airway obstruction is one of the hallmarks of asthma pathology. NETs may also stimulate airway SMCs proliferation and contribute to AHR and airway remodeling [16]. In addition, increasing evidence has indicated that nucleotide-binding oligomerization domain-like receptor family pyrin domain containing 3 (NLRP3) inflammasome activation plays a pivotal role in the pathogenesis of NA [15,17]. Assembly and activation of the NLRP3 inflammasome result in caspase-1-dependent release of IL-1β, thus leading to excessive inflammation and tissue damage [18]. Increased levels of NLRP3, caspase-1, and IL-1β were observed in the airways of NA [19]. Moreover, previous studies have demonstrated a link between the NLRP3 inflammasome and NETosis in severe asthma, and NETs can enhance IL-1β release by the activated NLRP3 inflammasome in neutrophils [15,20,21]. Consequently, neutrophils and neutrophil-derived NETs are involved in the initiation and propagation of NA, thus may serve as new therapeutic targets for NA.

Recently, various drugs have been evaluated in clinical trials for the treatment of asthma by targeting neutrophilic inflammation [22], such as macrolides and antibodies. Of note, macrolides can reduce the

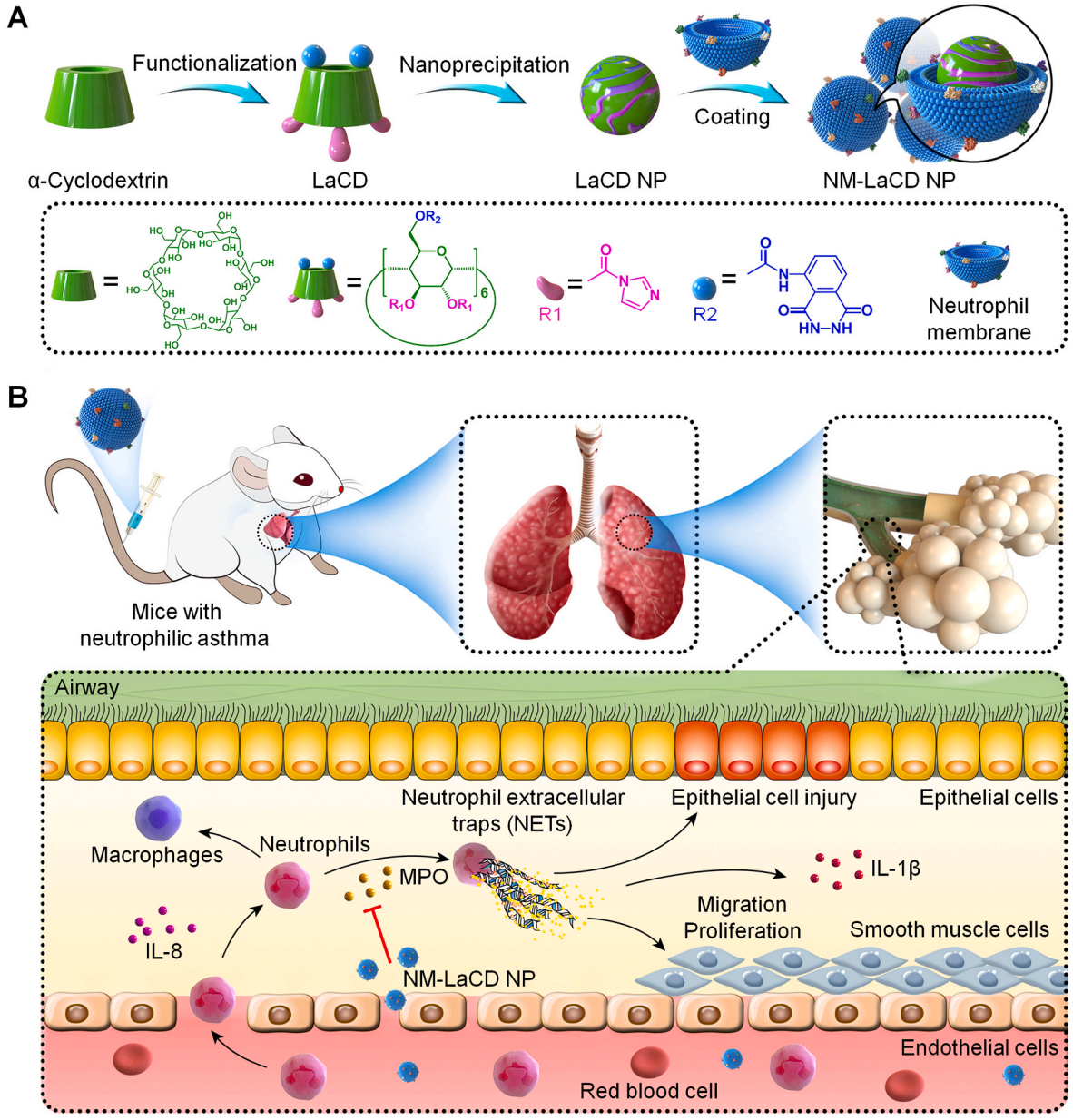

Fig. 1. Schematic illustration of engineering of multifunctional bioactive nanoparticles derived from a luminol-conjugated α-cyclodextrin (LaCD) material. (A) Chemical structure of LaCD as well as engineering of LaCD nanoparticles (LaCD NP) and neutrophil membrane-coated LaCD NP (NM-LaCD NP). (B) A sketch showing accumulation of NM-LaCD NP in the injured lungs and targeted treatment of neutrophilic asthma by regulating multiple pathologically relevant cells.

recruitment and activation of neutrophils, thereby attenuating neutrophilic inflammation-mediated airway injury [23,24]. However, increased resistance after long-term treatment and adverse reactions relevant to systemic distribution are still crucial concerns for this type of therapies [25]. For biological therapeutics like anti-IL-17R and anti-tumor necrosis factor (TNF)-α, whereas they are effective in treating NA by interfering pro-inflammatory signaling pathways [26], nonresponse in some patients and considerable side effects (such as serious infections and malignancies) have limited their clinical applications [27,28]. Therefore, both new therapies and innovative delivery strategies are necessary for safe and effective treatment of NA. Furthermore, in view of the direct contribution of abnormal airway epithelial cells and SMCs as well as their close relationship with neutrophilic inflammation, we reasonably hypothesize that agents capable of simultaneously regulating multiple target cells can serve as high potent drugs for NA.

Herein we proposed a multifunctional nanotherapy paradigm for the treatment of NA by regulating multiple pathologically relevant cells. As a proof of concept, nanoparticles (NPs) with multiple pharmacological activities were engineered using an intrinsically bioactive material LaCD (Fig. 1A). Both targeting and therapeutic effects of the engineered nanotherapy LaCD NP were examined in mice with induced NA after either intravenous or inhalation administration. To further enhance the targeting efficiency and efficacy of LaCD NP, a neutrophil cell membrane-based biomimetic strategy was applied. Moreover, multiple-cell-regulating mechanisms underpinning anti-asthmatic effects of LaCD NP were explored (Fig. 1B).

2. Experimental section

2.1. Synthesis and characterization of an α-cyclodextrin-derived material

A bioactive material, i.e., luminol-conjugated α-cyclodextrin (α-CD) (defined as LaCD) was synthetized as previously described [29,30]. Specifically, α-CD (0.68 g, 0.7 mmol) dried at 60 °C in vacuum overnight and 1,1′-carbonyldiimidazole (CDI) (0.68 g, 4.2 mmol) were co-dissolved in 6 mL of anhydrous DMF. The solution was magnetically stirred at 20–25 °C for 1.5 h, followed by precipitation in cold diethyl ether. The resulting CDI-activated α-CD (CDI-α-CD, 1.01 g) was dissolved in anhydrous DMF (8 mL), into which luminol (0.37 g, 2.1 mmol) and 0.1 mL of triethylamine were added, followed by reaction at 20–25 °C for additional 15 h under nitrogen. After precipitation from deionized water, the final product LaCD was collected by centrifugation and lyophilization. For materials characterization, ^{1}H NMR spectra were acquired on a spectrometer operating at 600 MHz (DD2, Agilent). Fourier-transform infrared (FT-IR) spectra were recorded on a PerkinElmer FT-IR spectrometer (100S, USA). UV–Vis spectroscopy was conducted on an ultraviolet spectrophotometer (TU-1901, Beijing Purkinje General instrument, China).

2.2. Fabrication of NPs based on LaCD

NPs based on LaCD (i.e., LaCD NP) were prepared by a nanoprecipitation method. In brief, 50 mg LaCD was dissolved in 2 mL of DMF, into which 10 mL of deionized water was slowly added. Then, the obtained mixture was incubated at room temperature for 2 h. Finally, LaCD NP was collected by centrifugation at 21000*g* and obtained by washing with deionized water 3 times. Through similar procedures, LaCD NPs containing Cy5 or Cy7.5 were fabricated.

2.3. Animals

All the animal care and experimental protocols were performed in agreement with the rules of the Animal Ethical and Experimental Committee of the Third Military Medical University (Army Medical University, Chongqing, China). BALB/c mice (18–22 g) were purchased from the Animal Center of the Third Military Medical University. All the animals were acclimatized to the laboratory for at least 7 days before experiments.

2.4. In vivo targeting of LaCD NP to the pulmonary tissue in mice with neutrophilic asthma

Neutrophilic asthma (NA) was established in mice as previously described [31]. In brief, on days 1 and 7, BALB/c mice were sensitized by intraperitoneal (i.p.) injection with 50 μg ovalbumin (OVA) in 50 μL of 0.01 M PBS (pH 7.4) mixed with 50 μL of 0.01 M PBS containing 2 mg $Al(OH)_3$ or the same volume of PBS. Immediately, each mouse was intranasally instilled with 100 μg OVA together with 10 μg lipopolysaccharide (LPS) in 50 μL of 0.01 M PBS or the same volume of PBS. Additionally, on days 14–18, all mice were challenged by exposure to an aerosolized 1% OVA solution (or 0.01 M PBS for the control mice) for 1 h. At 24 h after the final challenge, Cy7.5-labeled LaCD NP (Cy7.5/LaCD NP) was intravenously administered through the tail vein at 20 μg of Cy7.5 in each mouse. At 15 min post injection, mice were euthanized and perfused with PBS. Similarly, Cy5-labeled LaCD NP (Cy5/LaCD NP) at 60 μg of Cy5 was given to each mouse by aerosol inhalation. Meanwhile, saline was injected for control mice. Mice were euthanized and perfused with PBS at 6 h after aerosol inhalation. Then whole lungs were excised for ex vivo fluorescence imaging with an IVIS Spectrum system.

2.5. Cellular distribution of LaCD NP in lung tissues of asthmatic mice after intravenous (i.v.) injection or aerosol inhalation

Asthmatic mice were i.v. injected with Cy5/LaCD NP at 60 μg of Cy5 in each animal. Control mice were given with saline. At 1 h after administration, mice were euthanized. Whole lungs were isolated, minceded, and passed through a 40-μm nylon cell filter after red blood cells were depleted by incubation with ACK lysis buffer. The obtained cells were stained with APC/cyanine7-conjugated anti-mouse/human CD11b, PE-conjugated rat anti-mouse CD90, PE-conjugated rat anti-mouse Ly6G, FITC-conjugated anti-mouse F4/80, and BV421-conjugated rat anti-mouse CD326 for analysis by flow cytometry. In a separate study, lung sections were prepared and incubated with antibodies to Ly6G, EpCAM, CD90, and CD68 for 24 h, followed by incubation with the secondary antibody. After nuclei were stained with DAPI, confocal laser scanning microscopy (CLSM) images were acquired. Similarly, cellular distribution analysis of Cy5/LaCD NP was performed for lung tissues collected at 6 h after inhalation.

2.6. Efficacy of LaCD NP for the treatment of NA in mice after i.v. administration

NA in BALB/c mice was induced according to the aforementioned method. Mice were randomly assigned into four groups. On days 1 and 7, mice were sensitized with OVA and LPS. On days 14–18, all mice were challenged with 1% OVA for 1 h. For evaluation of therapeutic effects of LaCD NP, saline or LaCD NP (25 or 100 mg/kg) was given by i.v. administration at 1 h before the OVA challenge on days 14, 16, and 18. Meanwhile, in the normal control group, healthy mice were treated with saline. On day 19, mice were euthanized. Then 1 mL of PBS was injected into the lungs, and bronchoalveolar lavage fluid (BALF) was collected immediately. Subsequently, BALF was centrifuged at 450g and the obtained cells were labeled with APC-conjugated rat anti-mouse CD11b and PE-conjugated rat anti-mouse Ly6G antibodies for analysis by flow cytometry. In addition, 200 μL of Triton X-100 (0.3 wt%) was added into 1 mL of collected BALF and homogenized, followed by centrifugation at 16000*g* for 10 min at 4 °C. The levels of IL-17, myeloperoxidase (MPO), H_2O_2, tumor necrosis factor (TNF)-α, and IL-1β in the supernatant were quantified by ELISA. Also, blood samples were collected and the supernatant was obtained by centrifugation at 3000 rpm for 15 min at 25 °C. Serum levels of immunoglobulin E (IgE) were determined by ELISA. Furthermore, histological sections were prepared and stained

with hematoxylin and eosin (H&E), periodic acid-Schiff (PAS), Masson, or α-smooth muscle actin (α-SMA) antibody.

For evaluation of lung function, AHR was assessed as previously described [32]. In brief, mice were anesthetized by i.p. injection of 2% pentobarbital sodium, and then tracheostomized and intubated. Subsequently, mice were laid in a body plethysmograph chamber and the inserted tracheal tube was connected to the ventilator. Immediately, mice were challenged with methacholine at concentrations varying from 0, 3.125, 6.25, 12.5, to 25 mg/mL. The individual peak response value of resistance (R) was recorded. The results are represented as fold increases of R above baseline (R_L) and calculated as follows: $(R\text{-}R_L)/R_L$.

In addition, neutrophil counts and MPO levels in lungs were analyzed by immunofluorescence. In brief, lung sections were prepared and incubated with antibodies to Cy3-labeled Ly6G and FITC-labeled MPO. After nuclei were stained with DAPI, the sections were imaged by CLSM. Similarly, the formation of NETs in pulmonary tissues was analyzed by immunofluorescence after lung sections were incubated with antibodies to Cy3-labeled Ly6G and FITC-labeled citrullinated histone H3 (CitH3).

Also, the NLRP3 inflammasome activation in the lungs was evaluated. Specifically, lung tissues were grounded and cracked on ice for 30 min with RIPA containing PMSF. The supernatant was collected by centrifugation at 16000*g* for 10 min at 4 °C. Finally, RIPA lysate, sample loading buffer, and mercaptoethanol were used to adjust the protein concentration to 8 mg/mL, and the samples were boiled at 95 °C for 10 min to denaturate proteins. The expression of NLRP3, ASC, and procaspase-1 were detected by Western blotting (WB).

2.7. Therapeutic effects of LaCD NP in asthmatic mice by aerosol inhalation

Mice were randomly assigned into four groups. On days 1 and 7, mice were sensitized with OVA and LPS. LaCD NP at 1 or 5 mg/kg was given by aerosol inhalation. After 1 h, all mice were challenged with 1% OVA for 1 h on days 14–18. Asthmatic mice treated with saline served as the positive control. On day 19, BALF was collected for quantification of IL-17, neutrophils, MPO, H_2O_2, TNF-α, and IL-1β. Blood samples were collected for quantification of serum levels of IgE. Histological sections were also prepared and stained with H&E, PAS, Masson, or α-SMA antibody. For evaluation of lung function, AHR was assessed according to the aforementioned method. In addition, neutrophil counts and MPO levels in lungs were analyzed by immunofluorescence.

2.8. Preparation of neutrophil cell membrane-coated LaCD NP

Neutrophil cell membranes (NMs) were isolated according to the previously reported method [33]. In brief, peritoneal neutrophils were sonicated at 42 kHz for 5 min and then frozen at −80 °C for 30 min, followed by thawing at room temperature for another 30 min. After centrifugation at 700*g* for 10 min at 4 °C, the supernatant was collected and then centrifuged at 14,000*g* for another 30 min. NMs were finally obtained from the bottom of solution. Subsequently, NMs were washed with 0.5 mM EDTA and collected by centrifugation at 14000*g* for 30 min at 4 °C. The membrane content was quantified using a BCA kit. To prepare neutrophil membrane vesicles (NMVs), NMs were sonicated at 42 kHz for 5 min and physically extruded through a mini-extruder with a 400-nm polycarbonate membrane for 10 passes. Neutrophil membrane-functionalized LaCD NP (NM-LaCD NP) was produced using a sonication-extrusion method [33]. For membrane coating, NMVs were mixed with LaCD NP at a membrane protein-to-LaCD weight ratio of 1:1. The mixture was then sonicated with a bath sonicator for 5 min and physically extruded with a 200-nm polycarbonate membrane.

2.9. In vivo targeting effects and biodistribution profiles of NM-LaCD NP in asthmatic mice

NA in BALB/c mice was induced according to the aforementioned method. At 24 h after the final challenge, Cy5/LaCD NP or Cy5-labeled NM-LaCD NP (Cy5/NM-LaCD NP) was i.v. administered through the tail vein at 1.6 μg of Cy5 in each mouse. Meanwhile, saline was injected in the control mice. At 1 h post injection, mice were euthanized and perfused with PBS. Then whole lungs were excised for ex vivo fluorescence imaging with an IVIS Spectrum system. Also, other major organs including the heart, liver, spleen, and kidneys were excised for ex vivo imaging and quantitative analysis of the fluorescence intensities.

2.10. Therapeutic effects of NM-LaCD NP in asthmatic mice

Mice were randomly assigned into four groups. On days 1 and 7, mice were sensitized with OVA and LPS. On days 14–18, all mice were challenged with 1% OVA for 1 h. Either LaCD NP or NM-LaCD NP at 5 mg/kg was given by i.v. administration at 1 h before OVA challenge on days 14, 16, and 18. In the normal control group, healthy mice were treated with saline. On day 19, mice were euthanized and BALF was collected for quantification of neutrophils, IL-17, MPO, TNF-α, and IL-1β. Blood samples were collected for quantification of serum levels of IgE. In addition, histological sections were prepared and stained with H&E, PAS, Masson, or α-SMA antibody.

2.11. Statistical analysis

Statistical analysis was performed with the software of SPSS12 using one-way ANOVA with a multiple comparison method for experiments containing more than two groups. The one-way ANOVA with a two-tailed, unpaired *t*-test was performed for experiments with two groups. The $p < 0.05$ is considered to be statistically significant.

3. Results

3.1. Design, engineering, and characterization of bioactive cyclodextrin-derived NPs

As well documented, severe asthma is insensitive to corticosteroids that are generally used for asthma treatment [2,4,9]. Increasing evidence has indicated that neutrophils and neutrophil-derived NETs can directly contribute to the initiation, progression, and exacerbation of severe asthma [2,4–8,34]. Moreover, neutrophilic inflammation is closely associated with abnormal changes of macrophages, airway epithelial cells, and SMCs in the lungs, which are all responsible for the pathogenesis of asthma [2,3]. Consequently, we attempted to develop bioactive NPs for the treatment of severe asthma by regulating neutrophil-mediated inflammation and other target cells. To this end, a bioactive material LaCD was synthesized by conjugating luminol onto α-CD (Fig. 1A and Fig. S1A). α-CD, a cyclic oligosaccharide, was chosen as a scaffold compound, due to its multiple advantages, such as the excellent biosafety, well-defined chemical structure and composition, and abundant hydroxyl groups that can be easily functionalized by sophisticated chemistries [35–37]. FT-IR, ^{1}H NMR, and UV–Vis spectrometry revealed successful synthesis of LaCD (Figs. S1B–D). According to ^{1}H NMR and UV–Vis absorption spectra, approximately 1–2 luminol and 2–3 imidazole units were conjugated onto each LaCD molecule. Notably, the presence of relatively hydrophobic imidazole units afforded amphiphilicity to LaCD, thereby enabling self-assembly of LaCD in the absence of surfactants or stabilizers.

LaCD NP was prepared by direct nanoprecipitation of LaCD dissolved in DMF using deionized water as a poor solvent (Fig. 1A). Thus produced LaCD NP displayed well-defined spherical morphology, as illustrated by transmission electron microscopy (TEM), scanning electron microscopy (SEM), and atomic force microscopy (AFM) images (Fig. 2A–D).

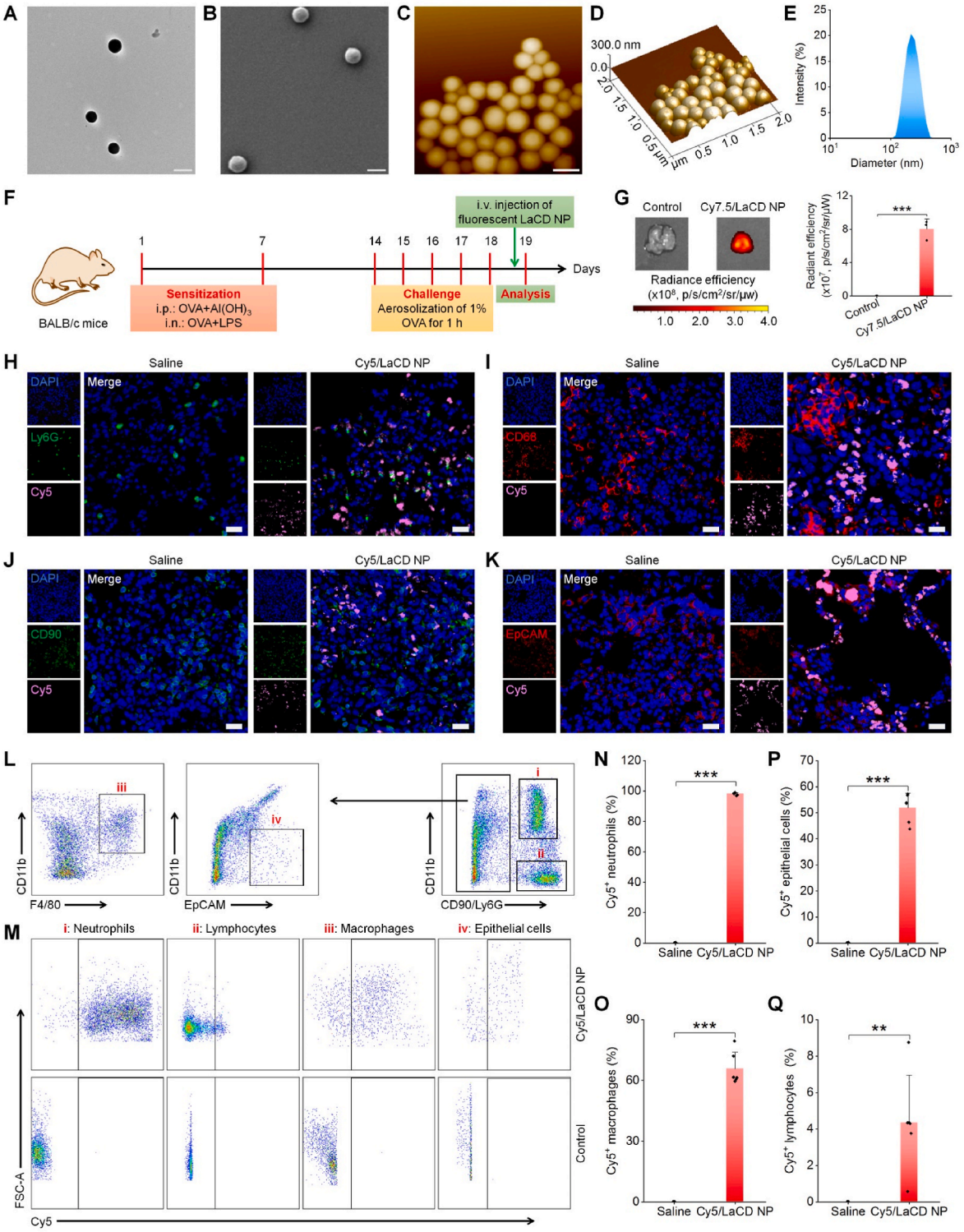

Fig. 2. Characterization of LaCD NP as well as lung targeting effects and cellular distribution patterns of LaCD NP after i.v. administration in NA mice. (A–E) TEM (A), SEM (B), and AFM (C–D) images as well as the size distribution profile (E) of LaCD NP. Scale bars, 300 nm. (F) Schematic illustration of experimental protocols. (G) Ex vivo fluorescence images (left) and quantitative data (right) indicate the lung accumulation of Cy7.5/LaCD NP at 15 min after i.v. injection at 20 μg of Cy7.5 in each NA mouse. (H–K) Immunofluorescence analysis of the distribution of Cy5/LaCD NP in different pulmonary cells. Cy5/LaCD NP at 60 μg of Cy5 was administered by i.v. injection in each mouse. The lung tissue sections were stained with Ly6G, CD68, CD90, and EpCAM antibodies for observation of neutrophils (H), macrophages (I), lymphocytes (J), and epithelial cells (K), respectively. Nuclei were stained with DAPI. Scale bars, 20 μm. (L–M) Cellular distribution of LaCD NP in lung tissues of NA mice after i.v. injection of Cy5/LaCD NP. (L) The gating strategy used for flow cytometry analysis of different lung cells. (M) Typical flow cytometric dot plots show Cy5 distribution in pulmonary cells of mice treated with saline or Cy5/LaCD NP. (N–Q) Quantified $Cy5^+$ cell populations in neutrophils (N), macrophages (O), pulmonary epithelial cells (P), and lymphocytes (Q). Biomarkers for neutrophils ($CD90/Ly6G^{high}CD11b^{high}$), macrophages ($CD90/Ly6G^{low}F4/80^{high}CD11b^{high}$), lung epithelial cells ($CD90/Ly6G^{low}EpCAM^{high}CD11b^{low}$), and lymphocytes ($CD90/Ly6G^{high}CD11b^{low}$) were separately used to distinguish different types of cells. Data are presented as mean ± SD (G, n = 3; N-Q, n = 6). *P < 0.05, **P < 0.01, ***P < 0.001.

Calculation based on AFM imaging showed that surface roughness of LaCD NP was approximately 0.31 ± 0.01, indicating low roughness. Surface roughness significantly affects the properties and functions of colloidal particles, and it also has considerable effects on interactions with different biomolecules [38]. According to previous findings, surface roughness can promote binding of biomolecules on NPs and enhance their cellular uptake [39]. Also, rough particles display large specific surface area, thereby showing increased absorption of proteins and other biomolecules [40]. Measurement by dynamic light scattering (DLS) revealed a relatively narrow size distribution profile for LaCD NP, with the mean diameter of about 226 ± 4 nm and ζ-potential of −11 ± 3 mV (Fig. 2E). LaCD NP displayed good colloidal stability in deionized water and a typical cell culture medium during 48 h of incubation, as implicated by slight variations in the mean diameter and ζ-potential (Figs. S2A–B). In addition, LaCD NP could be gradually hydrolyzed upon incubation with H_2O_2, one of reactive oxygen species (ROS) that are overproduced under inflammatory conditions, exhibiting a dose-dependent profile (Fig. S2C). In the presence of ROS, the luminol unit of LaCD will be first hydrolyzed into an aminophthalic acid structure (Fig. S3A). Subsequently, intermediate α-CD derivatives containing two different N-substituted carbamates will be further cleaved to give rise to α-CD, 3-aminophthalic acid, and imidazole [29]. The hydrolyzed products were confirmed by ^{1}H NMR spectroscopy (Fig. S3B).

3.2. In vivo targeting capability of LaCD NP in NA mice after i.v. administration

We then examined the distribution profiles of LaCD NP in the injured lung after i.v. administration. NA in mice was established by sequentially sensitizing and challenging with OVA and LPS (Fig. 2F) [31,41]. At 15 min post i.v. injection of Cy7.5/LaCD NP, considerable fluorescence signals in the lung of asthmatic mice were observed (Fig. 2G). Of note, the highest average fluorescence intensity was detected in the lung, as compared to those in other typical major organs (Figs. S4A–B). Estimation based on total fluorescent signals in different organs indicated that the lung targeting efficiency of i.v. administered LaCD NP was approximately 38.4 ± 6.8% (Fig. S4C), which was only lower than that in the liver (i.e., 57.9 ± 6.7%). This result indicated that LaCD NP can be effectively accumulated in the injured lung, largely resulting from a passive targeting effect via abundant alveolar capillaries in the lungs [30,37,42]. In addition, inflammation and oxidative stress can cause endothelial dysfunction and enhance the vascular permeability in the lungs, thereby further increasing the accumulation of LaCD NP in injured lung tissues of asthmatic mice [37]. Moreover, LaCD NP could be transported to the lung tissue by neutrophils and monocytes via their recruitment to the inflammatory site.

Furthermore, the distribution patterns of i.v. delivered LaCD NP in pulmonary cells were investigated. Immunofluorescence analysis revealed the localization of Cy5/LaCD NP in $Ly6G^+$ neutrophils, $CD68^+$ macrophages, $CD90^+$ lymphocytes, and $EpCAM^+$ epithelial cells in the lungs of asthmatic mice (Fig. 2H–K). In particular, a relative high distribution of Cy5/LaCD NP in neutrophils, macrophages, and epithelial cells was observed. Cellular localization profiles of Cy5/LaCD NP in the lung tissue were further quantified by flow cytometry (Fig. 2L-M). It was found that the Cy5/LaCD NP-positive cell proportion was 98.3 ± 0.9%, 65.8 ± 8.1%, 52.0 ± 5.6%, and 4.4 ± 2.6% for neutrophils, macrophages, lung epithelial cells, and lymphocytes, respectively (Fig. 2N-Q). Among all Cy5-positive lung cell populations, 63.5 ± 13.1% of them were neutrophils. These results demonstrated that i.v. delivered LaCD NP can efficiently target pulmonary inflammatory cells and epithelial cells that are all relevant to the pathogenesis of asthma [3], showing particularly high distribution in neutrophils.

3.3. Therapeutic effects of LaCD NP in NA mice after i.v. administration

Then we examined therapeutic benefits of LaCD NP in asthmatic mice. NA in mice was induced according to the aforementioned method, LaCD NP at 25 or 100 mg/kg was administered by i.v. injection at 1 h before the OVA challenge at days 14, 16, and 18 (Fig. 3A). At 24 h after different treatments, the serum level of IgE, a representative biomarker of asthma, significantly increased in saline-treated NA mice (Fig. 3B). By contrast, IgE levels markedly decreased after treatment with LaCD NP at either 25 or 100 mg/kg. Also, LaCD NP therapy significantly reduced the infiltration of neutrophils in the lung (Fig. 3C–D), in a dose-response manner. In addition, increased levels of MPO and H_2O_2, which are related to the neutrophil activation, were found in the pulmonary tissue of saline-treated asthmatic mice (Fig. 3E–F), while treatment with LaCD NP effectively decreased both MPO and ROS levels. Decreased neutrophil infiltration and MPO expression were confirmed by immunofluorescence analysis (Fig. S5). Furthermore, typical pro-inflammatory cytokines, including TNF-α, IL-1β, and IL-17 were also significantly reduced after treatment with LaCD NP (Fig. 3G–I). Of note, IL-17 released from Th17 cells is closely associated with neutrophilic inflammation in asthma [43]. The increased airway resistance is one of the hallmarks of asthma, which is also responsible for many symptoms during asthma exacerbations [3]. Whereas mice in the model group showed significantly higher AHR upon challenging with various doses of methacholine, both LaCD NP groups displayed notably attenuated airway resistance (Fig. 3J).

Moreover, examination on H&E-stained histological sections of lung tissues revealed notably reduced inflammatory cell infiltration and bronchial wall thicknesses in NA mice treated with LaCD NP (Fig. 3K). PAS staining of lung tissue sections indicated that both mucus secretion and goblet cell metaplasia were considerably inhibited by LaCD NP (Fig. 3L). Further inspection of lung sections stained with Masson or α-SMA showed airway remodeling in the model group, while this pathological change was effectively alleviated after treatment with LaCD NP (Fig. 3M − N). Collectively, these results demonstrated that treatment with LaCD NP via i.v. injection can efficaciously inhibit neutrophil-mediated inflammatory responses in the lung and alleviate the asthma severity.

3.4. Precision therapy of asthma in mice by inhaled LaCD NP

Inhalation has been considered as the most preferred drug delivery route for the treatment of pulmonary diseases [44], owing to its multiple advantages such as the large lung surface area, rapid absorption, high bioavailability, and lack of first-pass metabolism. Consequently, we further investigated targeting capability and therapeutic effects of inhaled LaCD NP in asthmatic mice. NA mice were established as aforementioned. At 24 h after the final challenge with OVA, Cy5/LaCD NP was delivered via aerosol inhalation (Fig. S6A). Ex vivo imaging of isolated lung tissues revealed strong fluorescence at 6 h after inhalation of Cy5/LaCD NP in asthmatic mice (Fig. S6B). Among the examined various major organs, we observed the strongest average fluorescence signal in the lungs (Figs. S6C–D), while extremely weak fluorescence was detected in other organs. According to total fluorescence intensities in different organs, the calculated lung targeting efficiency was 87.1 ± 2.8% (Fig. S6E), while the accumulation efficiency was 0.3 ± 0.1%, 7.6 ± 1.9%, 1.2 ± 0.3%, and 3.7 ± 1.8% for the heart, liver, spleen, and kidney, respectively. Consequently, inhalation of LaCD NP can afford a high selective accumulation in the lungs, mainly due to the large surface area and high permeability to deposited therapeutics [44–46]. Immunofluorescence analysis of lung sections showed co-localization of Cy5/LaCD NP with neutrophils, macrophages, lymphocytes, and epithelial cells (Figs. S7A–D), to varied degrees. Cellular distribution profiles of Cy5/LaCD NP in the lung tissue were further analyzed by flow cytometry (Figs. S7E–F). We found that 68.5 ± 12.2% neutrophils and 75.6 ± 23.6% macrophages were Cy5-positive (Figs. S7G–H). For epithelial cells and lymphocytes, the corresponding Cy5-positive cell proportion was 41.4 ± 24.3% and 2.1 ± 0.9%, respectively (Figs. S7I–J). In addition, we found that 63.3 ± 25.1% Cy5-positive cells

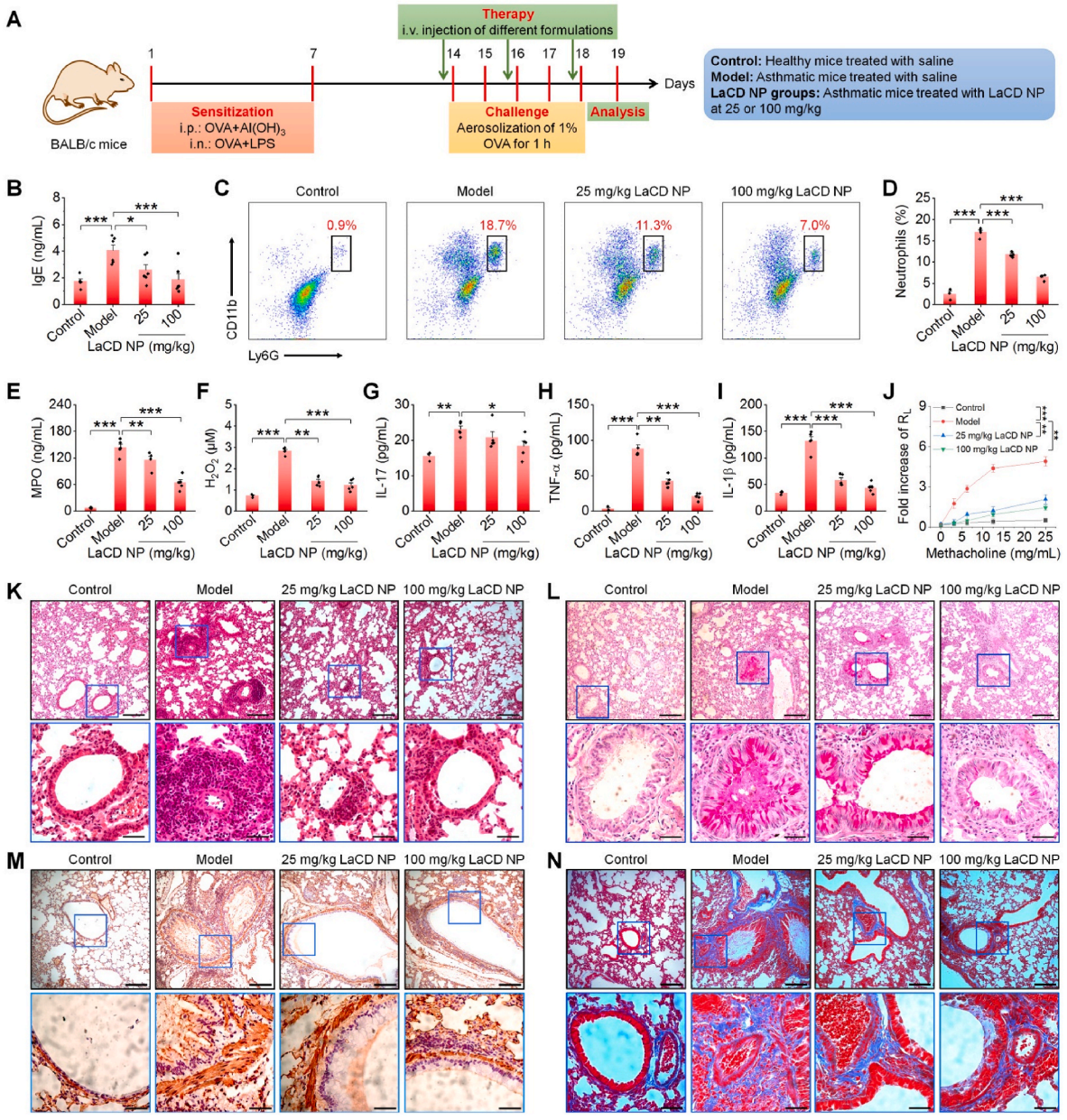

Fig. 3. Therapeutic effects of LaCD NP in asthmatic mice after i.v. injection. (A) Schematic illustration of experimental protocols. LaCD NP at 25 or 100 mg/kg was administered via i.v. injection at 1 h before the OVA challenge on days 14, 16, and 18. On day 19, mice were euthanized for therapeutic evaluations. (B) Serum levels of IgE. (C–D) Representative flow cytometric profiles (C) and quantitative analysis (D) of neutrophil counts in BALF. (E–F) Levels of MPO (E) and H_2O_2 (F) in BALF. (G–I) The expression levels of IL-17 (G), TNF-α (H), and IL-1β (I) in the BALF. (J) Changes in airway resistance. Mice were challenged with various doses of methacholine and treated with different formulations. (K–N) Histological sections of lung tissues stained with H&E (K), PAS (L), α-SMA antibody (M), or Masson (N). Scale bars: 100 μm (upper panels), 50 μm (lower panels). Data are presented as mean ± SD (B-J, n = 3–6). *P < 0.05, **P < 0.01, ***P < 0.001.

were neutrophils among all examined cell populations. Collectively, these results substantiated that inhaled LaCD NP can selectively accumulate in the lung and mainly distribute in neutrophils, macrophages, and epithelial cells, similar to the distribution patterns of i.v. delivered LaCD NP.

Subsequently, we examined therapeutic effects of inhaled LaCD NP in asthmatic mice. In this aspect, LaCD NP was administered at two theoretical doses 1 and 5 mg/kg by aerosol inhalation (Fig. 4A). After treatment with inhaled LaCD NP at 5 mg/kg, the serum level of IgE was significantly reduced (Fig. 4B). Also, inhalation treatment with LaCD NP dose-dependently and remarkably reduced the infiltration and activation of neutrophils in the lungs (Fig. 4C–F and Fig. S8), as implicated by significantly reduced MPO and ROS in BALF. Likewise, inhaled LaCD NP, particularly at 5 mg/kg, notably attenuated inflammatory responses and hyperresponsiveness in the lung airways (Fig. 4G–J). Further examination of pulmonary tissue sections stained with H&E or PAS indicated that airway inflammation, lung tissue damage, and airway mucus hypersecretion were effectively alleviated by inhalation treatment with LaCD NP, especially at 5 mg/kg (Fig. 4K-L). Moreover, airway remodeling was notably mitigated by inhaled LaCD NP, as implied by Masson and α-SMA staining of lung sections (Fig. 4M–N). These findings unambiguously evidenced the desirable therapeutic benefits of inhaled LaCD NP in NA mice. Compared to i.v. administration, inhalation therapy showed rapid onset of action. Importantly, inhaled LaCD NP was efficacious in the examined mouse model of asthma even at an extremely low theoretical dose of 1 mg/kg.

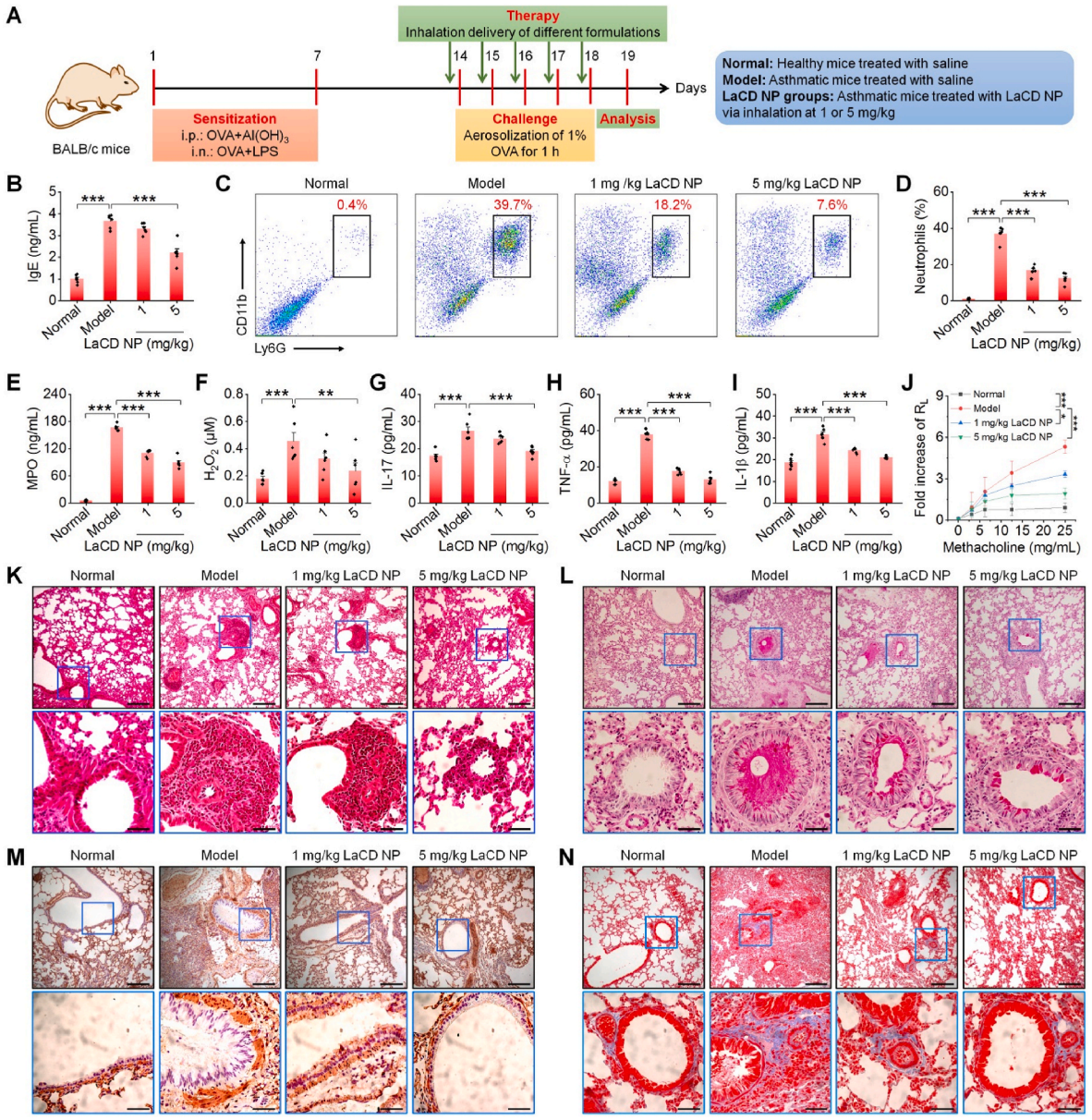

Fig. 4. Inhaled LaCD NP mitigates NA in mice. (A) A workflow shows regimens for the establishment of NA in mice and treatment regimens by inhalation of LaCD NP. For evaluation of therapeutic effects, LaCD NP was inhaled at theoretical doses of 1 or 5 mg/kg at 1 h before the OVA challenge on days 14–18. On day 19, mice were euthanized for analyses. (B) Serum levels of IgE. (C–D) Representative flow cytometric profiles (C) and quantitative analysis (D) of neutrophil counts in BALF. (E–F) Levels of MPO (E) and H_2O_2 (F) in BALF. (G–I) The expression levels of IL-17 (G), TNF-α (H), and IL-1β (I) in BALF. (J) Changes in airway resistance. Mice were treated with different formulations and challenged with various does of methacholine. (K–N) Histological sections of lung tissues stained with H&E (K), PAS (L), α-SMA antibody (M), or Masson (N). Scale bars: 100 μm (upper panels), 50 μm (lower panels). Data are presented as mean ± SD (B–I, n = 6; J, n = 5). *P < 0.05, **P < 0.01, ***P < 0.001.

3.5. Amplified targeting and therapeutic effects of neutrophil membrane-decorated LaCD NP in NA mice

Based on the above promising findings, we explored whether therapeutic effects of LaCD NP can be further improved by enhancing its targeting capability. Previously, both neutrophil-derived nanovehicles and neutrophil membrane (NM)-coated nanoparticles have been investigated for targeted delivery of therapeutic agents against different acute and chronic inflammatory diseases [47–49], showing desirable efficacies in preclinical studies. As a conceptual proof study, decoration via NM was performed for LaCD NP, to take advantage of the inflammatory site infiltration capability of neutrophils. Peritoneal neutrophils were first isolated from mice, showing a purity of approximately 90% and typical polymorphonuclear morphology (Fig. S9). NM was then prepared and coated onto LaCD NP by sonication and extrusion (Fig. 5A) [33]. Thus obtained NM-coated LaCD NP (i.e., NM-LaCD NP) had a uniform spherical core-shell structure, and a single neutrophil membrane layer was observed by TEM (Fig. 5B–C). Compared with uncoated LaCD NP, the mean diameter of NM-LaCD NP increased by approximately 20 nm (Fig. 5D). After NM coating, the ζ-potential value of NM-LaCD NP was reduced, which was comparable to that of NM (Fig. 5E). Moreover, Coomassie blue staining indicated the presence of NM-associated proteins on NM-LaCD NP (Fig. 5F). These data collectively suggested that NM was successfully coated onto the surface of LaCD NP.

Then in vivo targeting capability of NM-LaCD NP was evaluated using Cy5/NM-LaCD NP. Compared with the control Cy5/LaCD NP, ex vivo imaging showed significantly higher fluorescent signals for Cy5/

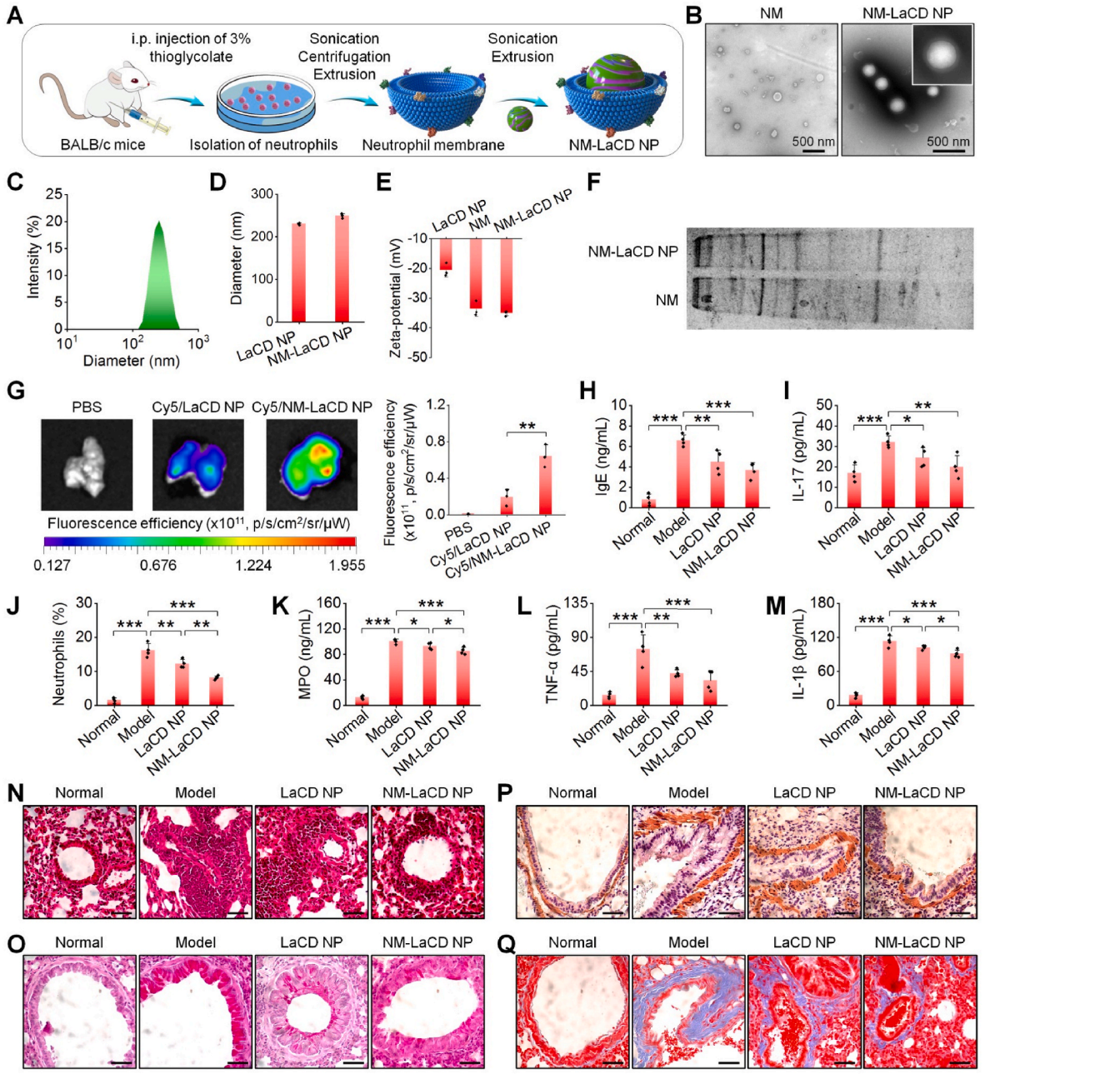

Fig. 5. Targeting therapy of NA by neutrophil membrane-functionalized LaCD NP (NM-LaCD NP) in mice. (A) Schematic illustration of engineering of NM-LaCD NP. (B) TEM images of neutrophil membrane (NM) and NM-LaCD NP. (C) The size distribution profile of NM-LaCD NP. (D–E) The mean diameter (D) and ζ-potential value (E) of LaCD NP and NM-LaCD NP. (F) Analysis of neutrophil membrane-associated proteins on NM and NM-LaCD NP by electrophoresis. (G) Ex vivo images (left) and quantified fluorescence intensities (right) showing the enhanced accumulation of Cy5/NM-LaCD NP in lung tissues after i.v. administration in NA mice. (H–I) Serum levels of IgE (H) and the expression levels of IL-17 in BALF (I) after different treatments. (J) Quantitative analysis of neutrophil counts in BALF. (K–M) Levels of MPO (K), TNF-α (L), and IL-1β (M) in BALF. (N–Q) Histological sections of lung tissues stained with H&E (N), PAS (O), α-SMA antibody (P), or Masson (Q). Scale bars, 50 μm. Data are presented as mean ± SD (D, E, G, n = 3; H–N, n = 4). *P < 0.05, **P < 0.01, ***P < 0.001.

NM-LaCD NP in the lung at 1 h after i.v. injection (Fig. 5G), which should be attributed to tropism of NM for inflammatory sites in the lung. As demonstrated by previous studies, cell membrane-coated NPs own some functions similar to the source cells, thus possessing the disease-relevant targeting capacity [33,47–50]. Correspondingly, Cy5/NM-LaCD NP displayed notably low accumulation in other major organs such as the heart, liver, spleen, and kidney, in comparison to Cy5/LaCD NP (Fig. S10). Consequently, the lung targeting performance of LaCD NP in NA mice can be effectively increased by surface engineering with the neutrophil-derived cell membrane.

Subsequently, in vivo therapeutic effects of NM-LaCD NP were examined in asthmatic mice. After i.v. administration at 5 mg/kg, NM-LaCD NP more effectively reduced the levels of serum IgE and IL-17 in BALF as well as more significantly attenuated neutrophil infiltration and neutrophil-mediated inflammatory responses in lung airways, as compared to LaCD NP (Fig. 5H-M and Fig. S11). In addition, histological analyses of lung sections revealed more desirable therapeutic outcomes of NM-LaCD NP, as implicated by notably suppressed airway inflammation, mucus secretion, lung tissue damage, and airway remodeling (Fig. 5N-Q and Fig. S12). Therefore, in vivo efficacies of the nanotherapy LaCD NP can be further potentiated by surface functionalization with the cell membrane.

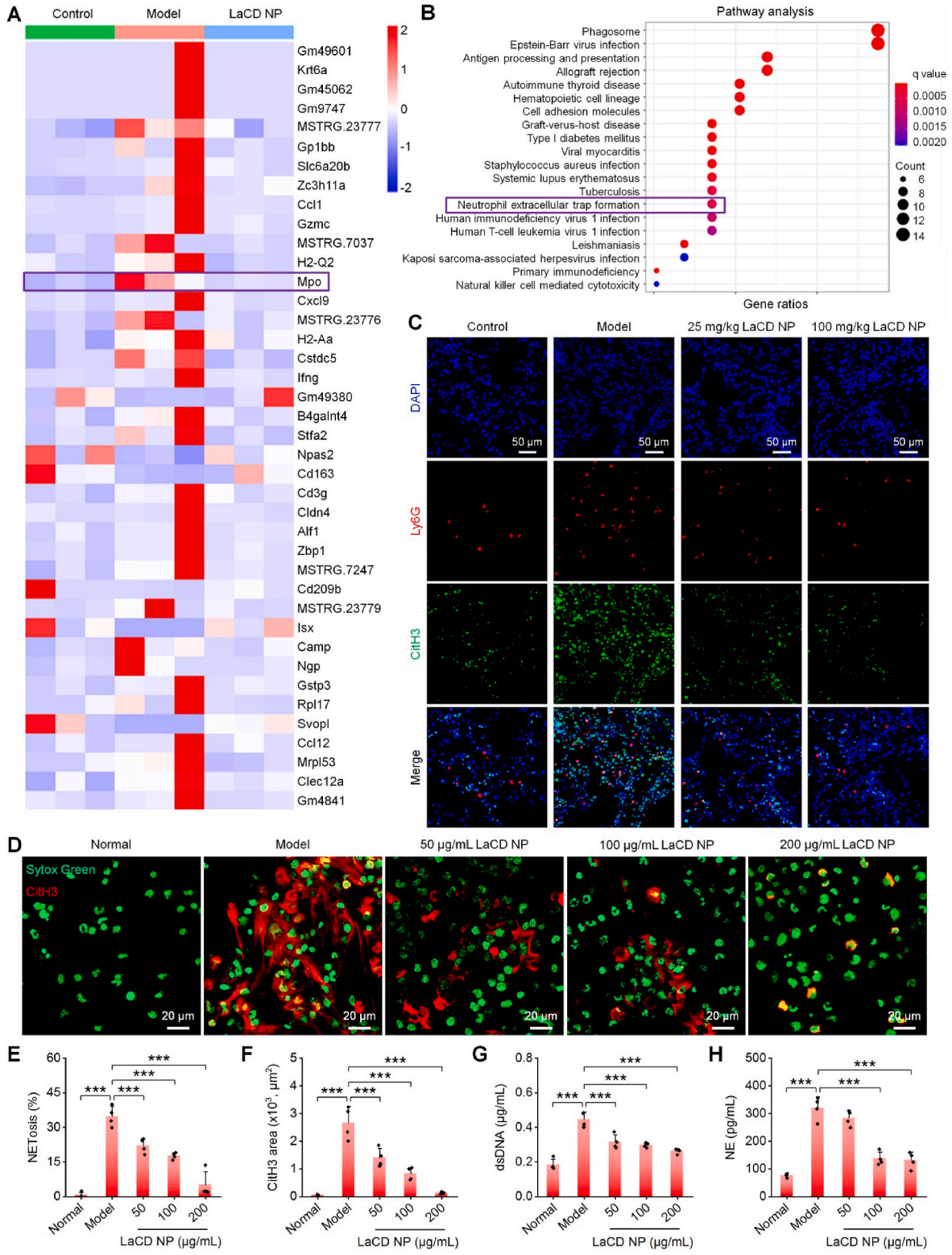

Fig. 6. Inhibition of the NETs formation by LaCD NP. (A) Heatmap shows clustered differential gene expression based on transcriptomic analysis of lung tissues from healthy or NA mice with or without treatment with LaCD NP by i.v. administration at 100 mg/kg. (B) KEGG enrichment bubble diagrams. (C) Immunofluorescence analysis of neutrophils and NETs in lung tissues from asthmatic mice after treatment with LaCD NP at 25 or 100 mg/kg. The lung tissue sections were stained with Cy3-Ly6G antibody (red) and FITC-CitH3 antibody (green) for detection of neutrophils and NETs, respectively. Nuclei were counterstained with DAPI. (D) Typical fluorescence images show the NETs formation by neutrophils after separate treatment with free medium (normal), PMA alone (model), or the combination of PMA and LaCD NP. dsDNA was stained with Sytox Green (green), while CitH3 was stained with Cy3 (red). Scale bars, 20 μm. (E–H) Quantitative analysis of the NETosis degree (E) and CitH3 area (F) as well as levels of dsDNA (G) and NE (H) in PMA-activated neutrophils after different treatments. Data are presented as means ± SD (E-H, n = 4). ***P < 0.001.

3.6. Mechanistic studies on anti-asthmatic effects of LaCD NP

3.6.1. In vitro cellular uptake and anti-inflammatory effects of LaCD NP in neutrophils

Further in vitro and in vivo studies were performed to examine mechanisms underlying anti-asthmatic effects of LaCD NP. First, CLSM observation and flow cytometric quantification revealed efficient endocytosis of Cy5/LaCD NP by mouse peritoneal neutrophils, in both time and dose dependent manners (Figs. S13–14). Even after 5 min of incubation, considerable cellular uptake of Cy5/LaCD NP by neutrophils was observed. We then investigated anti-inflammatory effects of LaCD NP in neutrophils. Mouse peritoneal neutrophils stimulated with phorbol 12-myristate 13-acetate (PMA) expressed a high level of MPO (Fig. S15A), indicating the activation of neutrophils. Also, typical pro-inflammatory cytokines, such as TNF-α and IL-1β were significantly increased in PMA-activated neutrophils (Figs. S15B–C). By contrast, treatment with LaCD NP dose-dependently inhibited the expression of these pro-inflammatory mediators in PMA-stimulated neutrophils. These results suggested that LaCD NP can effectively attenuate neutrophilic inflammation.

3.6.2. LaCD NP attenuates NETosis in vivo and in vitro

To further explore molecular mechanisms dominating pharmacological activities of LaCD NP, RNA-sequencing analysis was performed for lung tissues isolated from mice subjected to different treatments. Compared with the control group (i.e., healthy mice), the model group of saline-treated NA mice showed 125 up-regulated genes and 14 down-regulated genes, which were considerably reversed after treatment with i.v. delivered LaCD NP (Fig. 6A). Of note, among these differentially expressed genes (DEGs), the Mpo gene is one of most significantly varied genes before and after treatment with LaCD NP. As well documented, MPO is one of the most abundant proteins in neutrophils, and its expression is intimately associated with the neutrophil activation and subsequent formation of NETs [51], while NETs may positively contribute to the initiation and progression of NA [13]. Further KEGG enrichment analysis revealed the considerable contribution of the NETs signaling pathway to therapeutic effects of LaCD NP in asthmatic mice (Fig. 6B). Accordingly, we reasonably speculate that LaCD NP mainly alleviates NA by attenuating NETosis.

In support of this hypothesis, immunofluorescence analysis of lung tissues clearly revealed the presence and notable co-expression of Ly6G and CitH3 in the model group, indicating the NETs formation (Fig. 6C). After LaCD NP therapy, NETs in the lung tissues were notably reduced. In line with this finding, in vitro treatment with LaCD NP effectively inhibited PMA-mediated NETosis in neutrophils (Fig. 6D–F), as indicated by the remarkably decreased CitH3 expression and NETosis degree. This result was further confirmed by quantitative analysis of the contents of dsDNA and neutrophil elastase (NE) (both dsDNA and NE are major components of NETs) in PMA-stimulated neutrophils with or without treatment with LaCD NP (Fig. 6G–H). Together, these results demonstrated that LaCD NP can effectively inhibit NETosis, mainly by attenuating neutrophil recruitment and suppressing the expression of MPO by activated neutrophils.

3.6.3. Effects of LaCD NP on the NLRP3 inflammasome activation

Previous studies indicated that NETs can mediate the inflammasome activation and IL-1β release [15]. In addition, inflammasome-mediated, IL-1β-dependent responses are closely associated with the initiation and amplification of airway inflammatory processes and severe, steroid-resistant asthma [15,17]. Our results showed that LaCD NP effectively inhibited the expression of IL-1β by activated neutrophils (Fig. S15C). In view of the anti-NETosis activity of LaCD NP, we further examined whether LaCD NP can attenuate the NETs-mediated inflammasome activation. WB analyses revealed significantly increased expressions of NLRP3, ASC (an adapter protein), and pro-caspase-1 by NETs-induced neutrophils (Figs. S16A–D), indicating the formation of the NLRP3 inflammasome. Correspondingly, we also detected significantly increased IL-1β production by NETs-stimulated neutrophils (Fig. S16E), resulting from NLRP3 inflammasome-mediated activation of caspase-1 and promoted maturation of an inactive precursor of IL-1β (i.e., pro-IL-1β) [52]. By contrast, treatment with LaCD NP dose-dependently attenuated the formation and activation of the NLRP3 inflammasome in NETs-stimulated neutrophils, as implicated by significantly decreased NLRP3, ASC, pro-caspase-1, and IL-1β. Moreover, LaCD NP directly inhibited the formation and activation of the NLRP3 inflammasome in neutrophils induced with LPS and ATP (Figs. S16F–J). Agreeing with these in vitro findings, we also found the NLRP3 inflammasome activation in lung tissues from asthmatic mice (Fig. S17), which was notably inhibited after therapy with LaCD NP. Taken together, these results suggested that LaCD NP can effectively attenuate the formation and activation of the NLRP3 inflammasome in pulmonary neutrophils by its direct and indirect effects, thus alleviating NA.

3.6.4. In vitro anti-migration and anti-inflammatory effects of LaCD NP in macrophages

Previous studies demonstrated that neutrophils can induce adhesion and recruitment of monocytes/macrophages to the inflammatory site [53]. In addition, the production of pro-inflammatory cytokine IL-1β by activated macrophages can promote the development of NA [54]. Flow cytometric analysis revealed efficient internalization of LaCD NP by mouse peritoneal macrophages (Fig. S18). Transwell assay indicated that LaCD NP significantly suppressed migration of macrophages induced by either activated neutrophils or monocyte chemoattractant protein (MCP)-1 (Fig. 7A and Fig. S19), at all examined doses. Moreover, the expression level of IL-1β in activated macrophages could be significantly decreased after treatment with LaCD NP (Fig. 7B). These data suggested that LaCD NP can inhibit the recruitment and activation of macrophages mediated by activated neutrophils and other inflammatory mediators.

On the other hand, alveolar macrophages are the major lung-resident macrophages. In addition to maintaining tolerance and tissue homeostasis, they can initiate strong inflammatory responses [55]. CXC chemokines such as CXCL1 and CXCL2 (functional homologues of IL-8) produced by alveolar macrophages also induce the neutrophil migration [56]. We found significantly higher expression of CXCL1 by LPS-stimulated macrophages, as compared to normal macrophages (Fig. S20). Furthermore, CXCL1 released by macrophages could notably induce the migration of neutrophils (Fig. S21), while treatment with LaCD NP significantly reduced CXCL1 levels and suppressed the migration of neutrophils. Accordingly, LaCD NP can serve as an effective nanotherapy to attenuate neutrophil-mediated pro-inflammatory responses of macrophages. Moreover, cellularly internalized LaCD NP was able to directly inhibit pro-inflammatory effects of macrophages.

3.6.5. LaCD NP regulates pulmonary epithelial cells

Pulmonary epithelial cells also play an important role in the pathophysiology of asthma [57]. The normal airway epithelium is critical for defense, antigen presentation, and effective and quick innate responses to different allergens. In addition, airway epithelial cells can serve as an inflammatory initiator by producing pro-inflammatory mediators, in the presence of both exogenous and endogenous stimulators. IL-8, a potent neutrophil chemoattractant produced by epithelial cells, can facilitate the recruitment of neutrophils to the inflammatory site [12], while neutrophil adherence to lung epithelial cells further induces IL-8 release [58]. We found that LaCD NP can be effectively internalized by A549 lung epithelial cells (Fig. S22), well agreeing with in vivo cellular distribution profiles of LaCD NP in the lungs after either i.v. or inhalation administration (Fig. 2K and Fig. S7D). Consistently, LaCD NP effectively reduced the expression of IL-8 by LPS-stimulated pulmonary epithelial cells (Fig. S23). Correspondingly, LaCD NP was able to significantly suppress the migration of neutrophils induced by LPS-activated epithelial cells (Fig. S24).

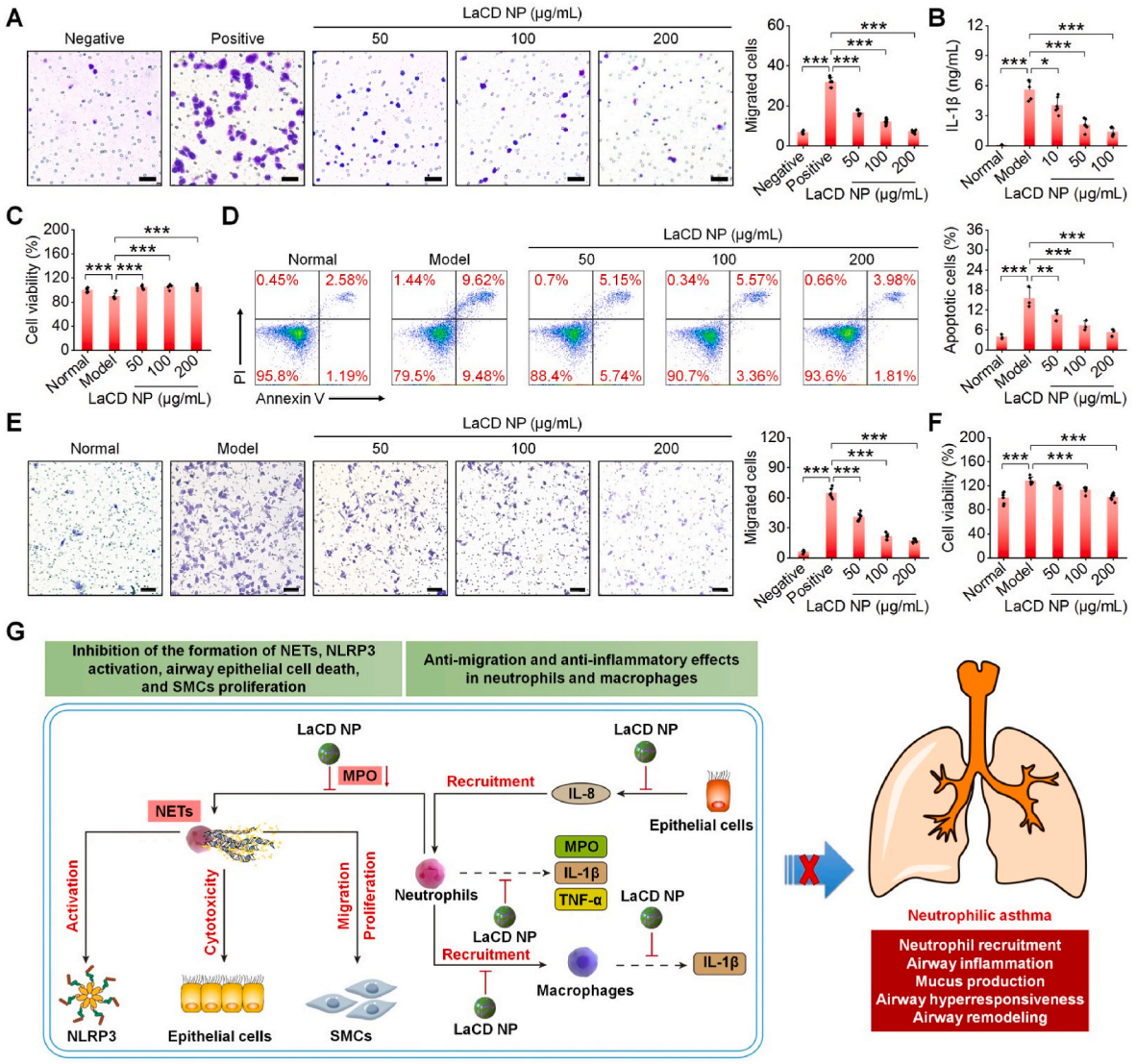

Fig. 7. LaCD NP suppressed neutrophil-mediated pro-inflammatory responses as well as inhibited airway epithelial cell death and SMCs proliferation. (A) In vitro suppression of neutrophil-mediated macrophage migration by LaCD NP. In the negative control group, RAW264.7 macrophages were treated with fresh medium, while the migration of macrophages was induced by activated neutrophils in the positive control group. Macrophages in other groups were simultaneously treated with neutrophils and various doses of LaCD NP. Scale bars, 100 μm. (B) The levels of IL-1β in peritoneal macrophages after separate treatment with fresh medium (normal), LPS/ATP alone (model), or the combination of LPS/ATP and various doses of LaCD NP. (C–D) LaCD NP reduced NET-induced apoptosis of epithelial cells. (E–F) LaCD NP inhibited the migration (E) and proliferation (F) of bronchial SMCs induced by NETs. In both cases, cells in the normal group were treated with free medium, while cells in the model group were incubated with NETs alone. LaCD NP groups were simultaneously treated with NETs and different concentrations of LaCD NP. Scale bars, 50 μm. (G) A sketch shows anti-asthmatic mechanisms of LaCD NP. Data are presented as means ± SD (A-B, E-F, n = 6; C, n = 5; D, n = 3). *P < 0.05, **P < 0.01, ***P < 0.001.

On the other hand, NETs can directly induce epithelial cell death, thereby promoting airway injury [13,14]. Also, NETs-derived NE may stimulate migration and proliferation of human bronchial SMCs, thus contributing to AHR and remodeling [16]. We found that LaCD NP effectively protected pulmonary epithelial cells from NETs-induced death (Fig. 7C–D). Also, LaCD NP significantly inhibited migration and proliferation of bronchial SMCs (Fig. 7E–F).

Taken together, the above results demonstrated that LaCD NP can inhibit the migration of neutrophils induced by activated airway epithelial cells, reduce neutrophil-mediated inflammatory responses, and attenuate the NETs formation and NLRP3 inflammasome activation in neutrophils. In addition, LaCD NP was able to mitigate neutrophil-induced pro-inflammatory responses of macrophages and prevent airway epithelial cell death and SMCs proliferation, thereby suppressing mucus production, airway remodeling, and hyperresponsiveness (Fig. 7G).

3.7. Safety evaluations of LaCD NP

Finally, safety profiles of LaCD NP were preliminarily tested. First, possible cytotoxicity of LaCD NP was assessed using neutrophils, A549 pulmonary epithelial cells, and human bronchial SMCs. Regardless of different cell types, high cell viability was found after incubation with various doses of LaCD NP, even at 1000 μg/mL (Fig. S25), indicating that LaCD NP exhibited low cytotoxicity for different pulmonary cells.

Further, acute toxicity of LaCD NP was evaluated after either i.v. or inhalation delivery. At days 1 and 3 after i.v. injection of LaCD NP at 1 g/kg, all treated mice showed normal behaviors and displayed similar body weight changes, when compared with saline-treated control mice (Fig. S26A). At day 14 after i.v. treatment, comparable organ index values were found for typical major organs (Fig. S26B). Quantification of representative hematological parameters showed no significant changes for LaCD NP-treated mice (Figs. S26C–F). Additionally, serum levels of

biomarkers related to liver and kidney functions were comparable for the saline and LaCD NP groups (Figs. S26G–J). Examination on H&E-stained histological sections of major organs revealed no distinguishable injuries and pathological variations for mice treated with LaCD NP (Fig. S27).

Similarly, we found no significant toxicity in mice after inhalation of LaCD NP at a theoretical dose of 50 mg/kg, as indicated by normal body weight changes and organ indices, insignificantly changed serum levels of hematological parameters and biomarkers relevant to liver/kidney functions, and histological analyses of sections of major organs (Figs. S28–29). After inhalation delivery, we also interrogated whether LaCD NP can cause inflammatory responses in the lung. In this case, we found no infiltration of inflammatory cells such as neutrophils and macrophages in BALF (Figs. S30A–D). Correspondingly, the levels of pro-inflammatory cytokines including TNF-α and IL-1β showed no significant changes, compared to saline-treated mice (Figs. S30E–F). Together, these preliminary results suggested that LaCD NP did not cause obvious systemic toxicity and pulmonary inflammation after i.v. or inhalation delivery at doses at least 10-fold higher than those used in therapeutic studies. This is in accordance with our finding that LaCD can be hydrolyzed into water-soluble compounds, including α-CD, 3-aminophthalic acid, and imidazole (Fig. S3), which can be easily excreted via the kidneys.

4. Discussion

NA, a severe, persistent, and fatal phenotype of asthma, is a major global health issue. Increasing evidence has suggested that the pathological role of neutrophilic inflammation in severe asthma is associated with un-resolving neutrophilia [4,8]. In particular, severe asthma is resistant to corticosteroid-based therapy, which is the standard treatment for asthma [2,4,8,9]. Also, other types of currently available drugs remain unsatisfied in the treatment of neutrophilic asthma, largely due to their limited pharmacological activities and considerable side effects resulting from nonspecific distribution after either systemic or local delivery (Table S1). Therefore both new therapies and site-specific delivery strategies need to be developed for efficient treatment of NA.

Herein we found that a bioactive material-derived nanotherapy LaCD NP can efficiently accumulate in the pulmonary tissue of NA mice after either i.v. injection or inhalation, largely by both passive targeting and inflammatory cell-mediated translocation effects. In both cases, the highest distribution of LaCD NP was found in the injured lungs, among all examined major organs. LaCD NP accumulated in the lungs mainly localized in neutrophils, macrophages, and epithelial cells, which are all intimately related to the pathogenesis of asthma [3]. Of note, LaCD NP displayed the highest distribution in neutrophils. For many nanotherapies, their efficient entry into cells is an important step toward desirable efficacies. Generally, NPs are internalized by cells via endocytosis [59], which occurs primarily in professional phagocytes, such as neutrophils and monocytes/macrophages. Also, other types of cells (e.g., endothelial cells and SMCs) have phagocytic activity [60]. Moreover, phagocytosis of NPs in the bloodstream can be initiated by adsorbing opsonins. Opsonized NPs are subsequently identified by specific receptors on phagocytic cells and internalized [61]. Similar to other NPs, LaCD NP in the bloodstream may be opsonized by immunoglobulins, complement proteins, or other plasma proteins. Then opsonized LaCD NP can be recognized by relevant receptors on the cell surface of neutrophils, macrophages, and epithelial cells, thereby leading to efficient cellular internalization.

In line with the desirable lung targeting efficiency, i.v. treatment of asthmatic mice with LaCD NP at either 25 or 100 mg/kg effectively reduced the serum level of IgE, pulmonary neutrophil infiltration, and BALF levels of pro-inflammatory cytokines relevant to neutrophilic inflammation and asthma. AHR of asthmatic mice was also significantly attenuated by LaCD NP. Consistently, therapy with i.v. delivered LaCD NP notably improved histological changes in the lungs of NA mice. Similar to i.v. administration, treatment of NA mice with LaCD NP via inhalation also afforded desirable therapeutic benefits. In this case, significant efficacies were even achieved at a theoretical inhalation dose of 1 mg/kg. Moreover, both targeting and therapeutic effects of LaCD NP can be significantly improved by decoration with neutrophil membrane. Consequently, LaCD NP was effective for NA after either i.v. or inhalation administration.

Mechanistically, LaCD NP effectively inhibited the neutrophil migration as well as infiltration and activation of neutrophils in the lungs, thereby notably attenuating neutrophil-mediated oxidative and inflammatory responses in asthmatic mice. As well demonstrated, both NETosis and inflammasome activation positively contribute to the initiation, progression, and exacerbation of asthma [19]. Further analyses showed that LaCD NP can remarkably prevent NETosis in vitro and in vivo. In addition, LaCD NP inhibited the formation and activation of the NLRP3 inflammasome in neutrophils either by reducing the NETs formation or via its direct effect. Accordingly, multiple pharmacological effects of LaCD NP on neutrophilic inflammation are responsible for its anti-asthmatic efficacy. Also, it has been reported that neutrophils can mediate the recruitment of macrophages to participate in the pathological process of NA [53]. We found that LaCD NP was able to inhibit the migration of macrophages induced by activated neutrophils and reduce the pro-inflammatory cytokine production in stimulated macrophages. Therefore, besides inhibition of neutrophil-mediated inflammatory responses of macrophages, LaCD NP can directly attenuate pro-inflammatory effects of macrophages, well agreeing with its cellular distribution in macrophages of the lungs.

As one of chemokines for neutrophils, IL-8 can promote the migration of neutrophils to the inflammatory site and play an important role in inflammation-associated airway diseases [12,62]. Importantly, elevated levels of IL-8 were detected in asthmatic patients [63]. We observed that LaCD NP can inhibit the secretion of IL-8 by pulmonary epithelial cells. LaCD NP also protected epithelial cells from NETs-induced death. In addition, LaCD NP effectively prevented the migration and proliferation of SMCs mediated by NETs. Notably, epithelial damage is a pathological feature of all asthma phenotypes [64], while migration and proliferation of SMCs mainly account for airway remodeling [65]. These data indicated that LaCD NP reduced airway obstruction and hyperresponsiveness largely by suppressing NETs-mediated pulmonary epithelial cell death and airway SMCs proliferation. Collectively, the potent anti-asthmatic activity of LaCD NP is attributed to its multiple pharmacological effects on pathologically relevant cells, including neutrophils, macrophages, epithelial cells, and SMCs.

Recently, small-molecule drugs or nucleic acids were loaded in NPs based on different materials (such as lipids and polymers) for targeted treatment of asthma (Table S2), demonstrating the effectiveness and advantages of NP-mediated targeting strategies. Nevertheless, the available nanocarriers can only target specific pulmonary cells other than all pathologically relevant cells, thereby resulting in limited cellular regulation effects. In addition, anti-asthmatic activity of these nanotherapies is mainly dominated by loaded therapeutic drugs that enable regulation of specific molecular or cellular targets, while the development and exacerbation of asthma are intimately associated with multiple cellular and molecular mediators. Moreover, complicated formulation procedures are generally involved in the development of these drug-loaded nanotherapies, which also negatively affect their further translation. Importantly, their efficacies for NA remain to be elucidated. Comparatively, our drug-free LaCD NP nanotherapies derived from an intrinsically bioactive material capable of simultaneously regulating multiple pathological cells can be facilely engineered with good quality control and low cost, thus holding great translation potential for precision therapy of NA.

5. Conclusion

In summary, we developed multi-bioactive nanotherapies for

targeted treatment of NA based on a cyclic oligosaccharide-derived bioactive material LaCD. After efficient accumulation in the injured lungs and distribution in pathologically relevant cells, LaCD NP showed desirable anti-asthmatic effects in mice, mainly by inhibiting the migration/infiltration of neutrophils as well as attenuating the NETs formation and NLRP3 inflammasome activation in neutrophils. Moreover, LaCD NP could suppress macrophage-mediated pro-inflammatory responses as well as mitigate airway epithelial cell death and SMCs proliferation, by preventing neutrophilic inflammation and its direct effects. Importantly, LaCD NP exhibited good in vivo safety performance after either i.v. administration or inhalation at doses at least 10-fold higher than that used for therapeutic studies. As a result, LaCD NP-based nanotherapies capable of simultaneously regulating multiple pathological cells are promising for precision treatment of NA, while the underlying design principle enables rational engineering of effective nanotherapies for other diseases associated with neutrophilic inflammation.

Ethics approval and consent to participate

All the animal care and experimental protocols were performed in agreement with the rules of the Animal Ethical and Experimental Committee of the Third Military Medical University (Army Medical University, Chongqing, China).

This work does not use human subjects.

CRediT authorship contribution statement

Jiajun Cai: Methodology, Investigation, Formal analysis, Validation, Writing – original draft, Writing – review & editing. **Hui Tao:** Methodology, Investigation, Formal analysis, Validation, Writing – original draft, Writing – review & editing. **Huan Liu:** Investigation, Validation. **Yi Hu:** Investigation, Validation. **Songling Han:** Investigation, Writing – original draft. **Wendan Pu:** Investigation, Writing – review & editing. **Lanlan Li:** Investigation. **Gang Li:** Investigation. **Chenwen Li:** Investigation. **Jianxiang Zhang:** Conceptualization, Writing – review & editing, Funding acquisition.

Declaration of competing interest

The authors declare that they have no known competing financial interests or personal relationships that could have appeared to influence the work reported in this paper.

Acknowledgements

This study was supported by the National Natural Science Foundation of China (Nos. 81971727 and 32271451), the Program for Scientific and Technological Innovation Leader of Chongqing (No. CQYC20210302362), the Program for Distinguished Young Scholars of TMMU, and the Graduate Supervisor Team Program of Chongqing in 2022.

Appendix A. Supplementary data

Supplementary data to this article can be found online at https://doi.org/10.1016/j.bioactmat.2023.04.023.

References

[1] https://ginasthma.org/gina-reports/.
[2] S.T. Holgate, et al., Asthma, Nat. Rev. Dis. Primers 1 (2015), 15025.
[3] A. Papi, C. Brightling, S.E. Pedersen, H.K. Reddel, Asthma, Lancet 391 (2018) 783–800.
[4] A. Ray, J.K. Kolls, Neutrophilic inflammation in asthma and association with disease severity, Trends Immunol. 38 (2017) 942–954.
[5] C. Radermecker, R. Louis, F. Bureau, T. Marichal, Role of neutrophils in allergic asthma, Curr. Opin. Immunol. 54 (2018) 28–34.
[6] J. Zhang, Z. Zhu, X. Zuo, H. Pan, J. Zheng, The role of NTHi colonization and infection in the pathogenesis of neutrophilic asthma, Respir. Res. 21 (2020) 170.
[7] J.R. Grunwell, S.T. Stephenson, R. Tirouvanziam, A. Lou, A.M. Fitzpatrick, Children with neutrophil-predominant severe asthma have proinflammatory neutrophils with enhanced survival and impaired clearance, J. Allergy Clin. Immunol. Pract. 7 (2018) 516–525, e516.
[8] A. Jatakanon, et al., Neutrophilic inflammation in severe persistent asthma, Am. J. Respir. Crit. Care Med. 160 (1999) 1532–1539.
[9] L.P. Boulet, H.K. Red De L, E. Bateman, S. Pe De Rsen, P.M. O'Byrne, The global initiative for asthma (GINA): 25 years later, Eur. Respir. J. 54 (2019), 1900598.
[10] E. Kolaczkowska, P. Kubes, Neutrophil recruitment and function in health and inflammation, Nat. Rev. Immunol. 13 (2013) 159–175.
[11] T. Nemeth, M. Sperandio, A. Mocsai, Neutrophils as emerging therapeutic targets, Nat. Rev. Drug Discov. 19 (2020) 253–275.
[12] L. Bo, et al., Pulmonary epithelial CCR3 promotes LPS-induced lung inflammation by mediating release of IL-8, J. Cell. Physiol. 226 (2011) 2398–2405.
[13] M. Uddin, H. Watz, A. Malmgren, F. Pedersen, Netopathic inflammation in chronic obstructive pulmonary disease and severe asthma, Front. Immunol. 10 (2019) 47.
[14] D. Pham, et al., Neutrophil autophagy and extracellular DNA traps contribute to airway inflammation in severe asthma, Clin. Exp. Allergy 47 (2017) 57–70.
[15] M.E. Lachowicz-Scroggins, et al., Extracellular DNA, neutrophil extracellular traps, and inflammasome activation in severe asthma, Am. J. Respir. Crit. Care Med. 199 (2019) 1076–1085.
[16] B. Salter, C. Pray, K. Radford, J.G. Martin, P. Nair, Regulation of human airway smooth muscle cell migration and relevance to asthma, Respir. Res. 18 (2017) 156.
[17] R. Kim, et al., Role for NLRP3 inflammasome-mediated, IL-1β-dependent responses in severe, steroid-resistant asthma, Am. J. Respir. Crit. Care Med. 196 (2017) 283–297.
[18] Schroder Kate, Jurg Tschopp, The inflammasomes, Cell 140 (2010) 821–832.
[19] J.L. Simpson, et al., Elevated expression of the NLRP3 inflammasome in neutrophilic asthma, Eur. Respir. J. 43 (2013) 1067–1076.
[20] X. Chen, Y. Li, L. Qin, R. He, C. Hu, Neutrophil extracellular trapping network promotes the pathogenesis of neutrophil-associated asthma through macrophages, Immunol. Invest. 50 (2021) 544–561.
[21] J. Campos, et al., Neutrophil extracellular traps and inflammasomes cooperatively promote venous thrombosis in mice, Blood Adv. 5 (2021) 2319–2324.
[22] J. De Volder, L. Vereecke, G. Joos, T. Maes, Targeting neutrophils in asthma: a therapeutic opportunity, Biochem. Pharmacol. 182 (2020), 114292.
[23] E.H.C. Wong, J.D. Porter, M.R. Edwards, S.L. Johnston, The role of macrolides in asthma: current evidence and future directions, Lancet Respir. Med. 2 (2014) 657–670.
[24] P.G. Gibson, P.S. Foster, Neutrophilic asthma: welcome back, Eur. Respir. J. 54 (2019), 1901846.
[25] S.L. Taylor, et al., Long-term azithromycin reduces haemophilus influenzae and increases antibiotic resistance in severe asthma, Am. J. Respir. Crit. Care Med. 200 (2019) 309–317.
[26] W.W. Busse, et al., Randomized, double-blind, placebo-controlled study of brodalumab, a human anti-IL-17 receptor monoclonal antibody, in moderate to severe asthma, Am. J. Respir. Crit. Care Med. 188 (2013) 1294–1302.
[27] Z.A. Borman, J. Côté-Daigneault, J.F. Colombel, The risk for opportunistic infections in inflammatory bowel disease with biologics: an update, Expert. Rev. Gastroent. 12 (2018) 1101–1108.
[28] S. Bonovas, et al., Biologic therapies and risk of infection and malignancy in patients with inflammatory bowel disease: a systematic review and network meta-analysis, Clin. Gastroenterol. Hepatol. 14 (2016) 1385–1397, e1310.
[29] H. Tao, et al., Luminescence imaging of acute liver injury by biodegradable and biocompatible nanoprobes, ACS Nano 14 (2020) 11083–11099.
[30] J. Guo, et al., A myeloperoxidase-responsive and biodegradable luminescent material for real-time imaging of inflammatory diseases, Mater. Today 20 (2017) 493–500.
[31] S. Zhao, et al., Lipopolysaccharides promote a shift from Th2-derived airway eosinophilic inflammation to Th17-derived neutrophilic inflammation in an ovalbumin-sensitized murine asthma model, J. Asthma 54 (2017) 447–455.
[32] R.H. Wilson, et al., Allergic sensitization through the airway primes Th17-dependent neutrophilia and airway hyperresponsiveness, Am. J. Respir. Crit. Care Med. 180 (2009) 720–730.
[33] Q. Zhang, et al., Neutrophil membrane-coated nanoparticles inhibit synovial inflammation and alleviate joint damage in inflammatory arthritis, Nat. Nanotechnol. 13 (2018) 1182–1190.
[34] H.S. Chang, et al., Neutrophilic inflammation in asthma: mechanisms and therapeutic considerations, Expet Rev. Respir. Med. 11 (2016) 29–40.
[35] J.X. Zhang, P.X. Ma, Cyclodextrin-based supramolecular systems for drug delivery: recent progress and future perspective, Adv. Drug Deliv. Rev. 65 (2013) 1215–1233.
[36] M.E. Davis, M.E. Brewster, Cyclodextrin-based pharmaceutics: past, present and future, Nat. Rev. Drug Discov. 3 (2004) 1023–1035.
[37] L. Li, et al., A broad-spectrum ROS-eliminating material for prevention of inflammation and drug-induced organ toxicity, Adv. Sci. 5 (2018), 1800781.
[38] A.E. Nel, et al., Understanding biophysicochemical interactions at the nano-bio interface, Nat. Mater. 8 (2009) 543–557.
[39] Y. Niu, et al., Nanoparticles mimicking viral surface topography for enhanced cellular delivery, Adv. Mater. 25 (2013) 6233–6237.

[40] C. Schulte, A. Podestà, C. Lenardi, G. Tedeschi, P. Milani, Quantitative control of protein and cell interaction with nanostructured surfaces by cluster assembling, Acc. Chem. Res. 50 (2017) 231–239.
[41] G.S. Whitehead, et al., Therapeutic suppression of pulmonary neutrophilia and allergic airway hyperresponsiveness by an RORγt inverse agonist, JCI Insight 5 (2019), e125528.
[42] E. Blanco, H. Shen, M. Ferrari, Principles of nanoparticle design for overcoming biological barriers to drug delivery, Nat. Biotechnol. 33 (2015) 941–951.
[43] N. Krishnamoorthy, et al., Neutrophil cytoplasts induce Th17 differentiation and skew inflammation toward neutrophilia in severe asthma, Sci. Immunol. 3 (2018), eaao4747.
[44] A.C. Anselmo, Y. Gokarn, S. Mitragotri, Non-invasive delivery strategies for biologics, Nat. Rev. Drug Discov. 18 (2019) 19–40.
[45] A. Kuzmov, T. Minko, Nanotechnology approaches for inhalation treatment of lung diseases, J. Contr. Release 219 (2015) 500–518.
[46] Y. Guo, et al., Pharmaceutical strategies to extend pulmonary exposure of inhaled medicines, Acta Pharm. Sin. B 11 (2021) 2565–2584.
[47] R.H. Fang, A.V. Kroll, W. Gao, L. Zhang, Cell membrane coating nanotechnology, Adv. Mater. 30 (2018), 1706759.
[48] H. Yan, et al., Engineering cell membrane-based nanotherapeutics to target inflammation, Adv. Sci. 6 (2019), 1900605.
[49] D. Chu, X. Dong, X. Shi, C. Zhang, Z. Wang, Neutrophil-based drug delivery systems, Adv. Mater. 30 (2018), 1706245.
[50] T. Kang, et al., Nanoparticles coated with neutrophil membranes can effectively treat cancer metastasis, ACS Nano 11 (2017) 1397.
[51] K.D. Metzler, et al., Myeloperoxidase is required for neutrophil extracellular trap formation: implications for innate immunity, Blood 117 (2011) 953–959.
[52] K.V. Swanson, M. Deng, J.P.Y. Ting, The NLRP3 inflammasome: molecular activation and regulation to therapeutics, Nat. Rev. Immunol. 19 (2019) 477–489.
[53] O. Soehnlein, L. Lindbom, C. Weber, Mechanisms underlying neutrophil-mediated monocyte recruitment, Blood 114 (2009) 4613–4623.
[54] K. Niemi, et al., Serum amyloid A activates the NLRP3 inflammasome via P2X7 receptor and a cathepsin B-sensitive pathway, J. Immunol. 186 (2011) 6119–6128.
[55] T. Hussell, T.J. Bell, Alveolar macrophages: plasticity in a tissue-specific context, Nat. Rev. Immunol. 14 (2014) 81–93.
[56] N. Mizutani, T. Nabe, S. Yoshino, IL-17A promotes the exacerbation of IL-33-induced airway hyperresponsiveness by enhancing neutrophilic inflammation via CXCR2 signaling in mice, J. Immunol. 192 (2014) 1372–1384.
[57] B.N. Lambrecht, H. Hammad, Allergens and the airway epithelium response: gateway to allergic sensitization, J. Allergy Clin. Immunol. 134 (2014) 499–507.
[58] S. van Wetering, S.P.G. Mannesse-Lazeroms, M.A.J.A. van Sterkenburg, P. S. Hiemstra, Neutrophil defensins stimulate the release of cytokines by airway epithelial cells: modulation by dexamethasone, Inflamm. Res. 51 (2002) 8–15.
[59] M.P. Stewart, et al., In vitro and ex vivo strategies for intracellular delivery, Nature 538 (2016) 183–192.
[60] S. Behzadi, et al., Cellular uptake of nanoparticles: journey inside the cell, Chem. Soc. Rev. 46 (2017) 4218–4244.
[61] M.J. Mitchell, et al., Engineering precision nanoparticles for drug delivery, Nat. Rev. Drug Discov. 20 (2021) 101–124.
[62] P.L.B. Bruijnzeel, M. Uddin, L. Koenderman, Targeting neutrophilic inflammation in severe neutrophilic asthma: can we target the disease-relevant neutrophil phenotype, J. Leukoc. Biol. 98 (2015) 549–556.
[63] Duy, et al., Association of autophagy related gene polymorphisms with neutrophilic airway inflammation in adult asthma, Korean J. Intern. Med. 31 (2016) 375–385.
[64] P.S. Hiemstra, P.B. McCray Jr., R. Bals, The innate immune function of airway epithelial cells in inflammatory lung disease, Eur. Respir. J. 45 (2015) 1150–1162.
[65] B. Camoretti-Mercado, R.F. Lockey, Airway smooth muscle pathophysiology in asthma, J. Allergy Clin. Immunol. 147 (2021) 1983–1995.